Biochemical and Biophysical Research Communications 613 (2022) 140–145

Contents lists available at ScienceDirect

Biochemical and Biophysical Research Communications

journal homepage: www.elsevier.com/locate/ybbrc

Estrogen and BRCA1 deficiency synergistically induce breast cancer mutation-related DNA damage

Jiahao Chen [a, c, 1], Jingxin Liu [a, c, 1], Pengguihang Zeng [c, 1], Cai Zhao [c, 1], Xinyi Liu [c], Jun Sun [c], Jia Wang [c, d], Peihang Fang [c], Wenjie Chen [a, **], Junjun Ding [a, b, c, e, *]

[a] Vaccine Research Institute, The Third Affiliated Hospital of Sun Yat-sen University, Sun Yat-sen University, Guangzhou, 510630, China
[b] Advanced Medical Technology Center, The First Affiliated Hospital, Zhongshan School of Medicine, Sun Yat-sen University, Guangzhou, 510630, China
[c] Department of Cell Biology, Zhongshan School of Medicine, Sun Yat-Sen University, Guangzhou, 510080, China
[d] Guangzhou Medical University-Guangzhou Institute of Biomedicine and Health Joint School of Life Sciences, Guangzhou Medical University, Guangzhou, 511436, China
[e] West China Biomedical Big Data Center, West China Hospital, Sichuan University, Chengdu, 610041, China

A R T I C L E I N F O

Article history:
Received 19 April 2022
Accepted 30 April 2022
Available online 2 May 2022

Keywords:
Breast cancer
BRCA1
Estrogen
DNA Damage
Estrogen receptor-α

A B S T R A C T

Estrogen (E2) is crucial for the development of breast cancer caused by *BRCA1* mutation, and can increase the DNA damage in BRCA1-deficient cells. However, the mechanisms through which BRCA1 deficiency and E2 synergistically induce DNA damage remains unclear. In this study, we analyzed the distribution of DNA damage in E2-treated BRCA1-deficient cells. We detected DNA lesions in the vicinity of genes that are transcriptionally activated by estrogen receptor-α (ER). Loss of BRCA1 altered chromatin binding by ER, which significantly affected the distribution of DNA damage. Moreover, these changes were associated with the established mutations in BRCA1-mutant breast cancer. Taken together, our findings reveal a new mechanism underlying the DNA damage in breast cancer cells that is synergistically induced by BRCA1 deficiency and E2.

1. Introduction

BRCA1 is a core DNA damage repair gene in homologous recombination repair (HR) pathway [1,2], and mutation of this gene leads to genomic instability and tumorigenesis. In addition, germline *BRCA1* mutations are associated with a higher risk of breast and ovarian cancers [2]. However, the mechanism underlying the highly tissue-specific oncogenic transformation induced by BRCA1 mutations. One possible explanation is that breast and ovarian epithelial cells are responsive to estrogen (E2) signaling during the normal menstrual cycle [2], and there is evidence that E2 promotes mammary tumor initiation and progression in BRCA1-deficient animal and PDX models [3].

Studies show that the genome instability caused by E2 may have a carcinogenic effect in case of a defective BRCA1-mediated HR repair pathway [4]. E2 induces DNA damage through various mechanisms, such as triggering oxidative stress through its metabolites [5], mediating R-loop formation [6], and inhibiting the DNA damage repair process [7,8]. In addition, BRCA1 can directly interact with estrogen receptor-α (ER) and inhibit its transcriptional activation in response to E2 [9]. Nevertheless, the mechanistic of DNA damage caused by the synergy of BRCA1 deficiency and E2 is poorly understood. Moreover, the distribution of these DNA lesions, and their association with clinical mutations in breast cancer are largely unclear.

In this study, we identified the chromatin distribution of E2-induced DNA damage in BRCA1-deficient breast cancer cells. We found that loss of BRCA1 altered chromatin binding of ER, which led to the redistribution of DNA lesions as well as the emergence of new lesions. Our findings also showed that E2 induces DNA damage through ER-activated transcription. Finally, there was significant correlation between the DNA lesions in the E2-stimulated *BRCA1*-deficient cells and the clinically relevant mutations in BRCA1-mutant breast cancer. These genes may serve as potential biomarkers and therapeutic targets for the treatment of BRCA1-mutant breast cancer.

* Corresponding author. Vaccine Research Institute, The Third Affiliated Hospital of Sun Yat-sen University, Sun Yat-sen University, Guangzhou, 510630, China.
** Corresponding author. Vaccine Research Institute, The Third Affiliated Hospital of Sun Yat-sen University, Sun Yat-sen University, Guangzhou, 510630, China.
E-mail addresses: chenwj5@mail.sysu.edu.cn (W. Chen), dingjunj@mail.sysu.edu.cn (J. Ding).
[1] These authors have contributed equally to this work and share first authorship.

https://doi.org/10.1016/j.bbrc.2022.04.142
0006-291X/

2. Materials and methods

2.1. Cell culture

Breast cancer cell line MCF7 was from Professor Hai Hu'lab at Sun Yat-sen university. MCF7 were cultured in RPMI 1640 medium supplemented with 10% fetal bovine serum (FBS) (VISTECH) and 1% penicillin-streptomycin (Hyclone). The MCF7 were infected by the lentivirus containing PLKO vector for knockdown of ER and BRCA1. The infected MCF7 were screened by 2 μg/ml puromycin for 5 days. All cells were cultured in 5% CO_2 37 °C incubator.

2.2. RNA isolation and RNA-seq

Total RNA was extracted from cell pellets using RNAzol reagent (MRC). Two replicates were used for RNA-seq experiments. RNA was quantified by Nanodrop 2000 (Thermo Fisher Scientific). Total RNA (5 μg) was supplied to Novogene, and sequencing was performed by NovaSeq 6000.

2.3. qRT-PCR analysis

mRNA was reverse-transcribed using a PrimeScript™ RT Master Mix (Takara) according to the manufacturer's protocol. Quantitative Real-time PCR was performed with the Roche 480 Lightcycler with SYBR qPCR Master Mix (Vazyme). Triplicate reactions were carried out for each sample. Individual gene expression was normalized to GAPDH. Primers sequences are listed in Supplement Table S1.

2.4. Immunofluorescence

Cells were plated on the 96-well cell culture plates (PerkinElmer #6055302). The cells were fixed using 4% paraformaldehyde for 15 min. Then cells were permeabilized by 0.5% Triton X-100 for 5 min. Cells were blocked with 100 μl blocking buffer (5% BSA, 0.5% Triton X-100, 94.5% PBS) for 60 min at room temperature. Primary antibody was added in blocking buffer at 4 °C overnight. Cells were washed with PBS followed by incubation with labeled secondary antibody 1:1000 in blocking buffer for 1 h at room temperature. Finally, images were acquired at Operetta CLS High Content Analysis System (PerkinElmer HH16000000).

2.5. ChIP-seq and data analysis

ChIP-seq was performed as previously described [10] in MCF7 with or without E2(10 nM) or DRB(5 μM) treatment for 12 h.

We aligned the ChIP-Seq data to the hg19 reference genome by bowtie2 with default parameter, followed by removing the multiple aligned reads, PCR duplications with samtools. We used macs2 to calling peaks with control, setting a q value cutoff of 0.05. The HOMER tool (http://homer.salk.edu/homer/motif/) was used to detect the motifs. The BEDtools is used to analyze .bed files (https://bedtools.readthedocs.io/en/latest/content/bedtools-suite.html).

2.6. RNA-seq data analysis

We aligned the RNA-seq data to the hg19 reference genome using STAR. Using HTSeq-count, we counted the uniquely mapped reads and transformed to TPM (Transcripts Per Kilobase Million) for further analyses. We detected the differentially expressed genes using edgeR. Genes were considered differentially expressed when the overall false discovery rate (FDR) < 0.05 and fold change is above 2.0.

2.7. GSEA analysis

GSEA (Gene Set Enrichment Analysis) are performed by GSEA software Windows version.

2.8. Circos plots

Circos plots are created by Circos following the tutorial. CNV profile was retrieved from UCSC Xena TCGA data portal (https://xenabrowser.net/datapages/?dataset=TCGA-BRCA.cnv.tsv&host=https%3A%2F%2Fgdc.xenahubs.net&removeHub=https%3A%2F%2Fxena.treehouse.gi.ucsc.edu%3A443), which containing genes with CNV in 44 Brca1-m breast cancer samples. Each chromosome was divided into 10 bins with equal length and count how many samples in which these bins containing CNVs. Each bin with a number of samples exceeding the average of all bins were defined as CNV hotspot regions. SNV and small InDel profile was also retrieved from UCSC Xena TCGA data portal which containing SNV and small InDel features in 40 Brca1-m breast cancer samples. Each bin with a density of SNVs and InDels exceeding the average of all bins were defined as SNV and InDel hotspot regions. CrossMap was used to convert genome build to hg19.

2.9. Standard statistical analysis

P values were determined using unpaired Student's *t*-test unless otherwise stated. Differences were considered statistically significant when $p < 0.05$ (*$p < 0.05$, **$p < 0.01$, ***$p < 0.001$). Data are shown as mean ± SD or SEM.

3. Results

3.1. E2-induced DNA damage in BRCA1-deficient cells is associated with ER

E2 is known to induce DNA damage in breast epithelial cells [4]. In line with previous reports, we found that the number of γH2AX foci increased significantly in the MCF7 cells upon E2 treatment (Fig. 1A and B). Furthermore, E2-induced accumulation of γH2AX foci was more pronounced in the BRCA1-knockdown cells (Fig. 1A and B; Supplementary Fig. 1A). Consistent with the IF results, ChIP-seq of γH2AX showed that the number of global γH2AX peaks were significantly higher in the E2-treated versus the untreated BRCA1-deficient breast cancer cells (Fig. 1C; Supplementary Figs. 1C–E). These results indicate that the loss of BRCA1 exacerbates E2-induced DNA damage. In addition, knocking down ER in the breast cancer cells (Supplementary Fig. 1B) significantly decreased the number of γH2AX foci in response to E2 (Fig. 1D and E), indicating that E2-induced DNA damage is dependent on ER. The ChIP-seq data further showed that DNA damage was more likely to occur at sites with strong ER binding (Fig. 1F). We further verified this result by ChIP-qPCR at the loci of *PTPFR* and *ZFHX3* (Supplementary Fig. 1F). These results suggest that the ER binding is correlated with the occurrence of DNA damage induced by BRCA1 deficiency and E2. Taken together, E2-induced DNA damage in BRCA1-knockdown breast cancer cells preferentially occurs in the ER-occupied genome regions.

3.2. DNA damage occurs at specific ER-binding sites in BRCA1-deficient cells

Previous studies have shown that BRCA1 inhibits ER-α signaling in mammary cell lines by directly interacting with ER [9,11]. To ascertain whether BRCA1 loss induces DNA damage by altering the ER transcriptional targets, we analyzed the ER binding sites in the

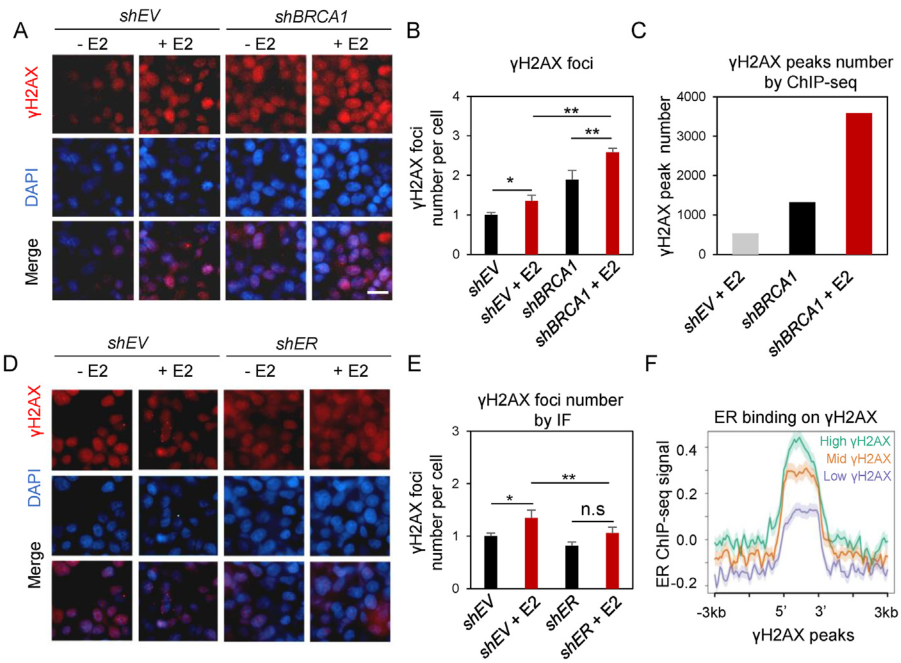

Fig. 1. DNA damage induced by E2 in BRCA1-deficient cell is associated with ER. (A) Representative immunostaining images of γH2AX in MCF7 cells infected with lentivirus-mediated empty vector (*shEV*) or BRCA1 short hairpin RNA (*shBRCA1*) with or without 10 nM estrogen (E2) treatment for 12 h (Red, γH2AX; blue, DAPI). Scale bars, 20 μm (B) Number of γH2AX foci per cell in the *shEV* or *shBRCA1* MCF7 cells with or without E2 (10 nM) treatment for 12 h (Red, γH2AX; blue, DAPI). (C) Number of γH2AX peaks in *shEV* or *shBRCA1* MCF7 cells with or without E2 (10 nM) treatment for 12 h. (D) Representative immunostaining images of γH2AX in *shEV* or *shER* MCF7 cells with or without E2 (10 nM) treatment for 12 h (Red, γH2AX; blue, DAPI). Scale bars, 20 μm (E) Number of γH2AX foci per cell in *shEV* or *shER* MCF7 cells with or without E2 (10 nM) treatment for 12 h (F) Average reads density plots for ER chromatin binding proximal to γH2AX peaks divided into high, mid and low peak strength in E2-treated (10 nM) *shBRCA1* MCF7 cells. The total number of γH2AX peaks was 3597. (For interpretation of the references to colour in this figure legend, the reader is referred to the Web version of this article.)

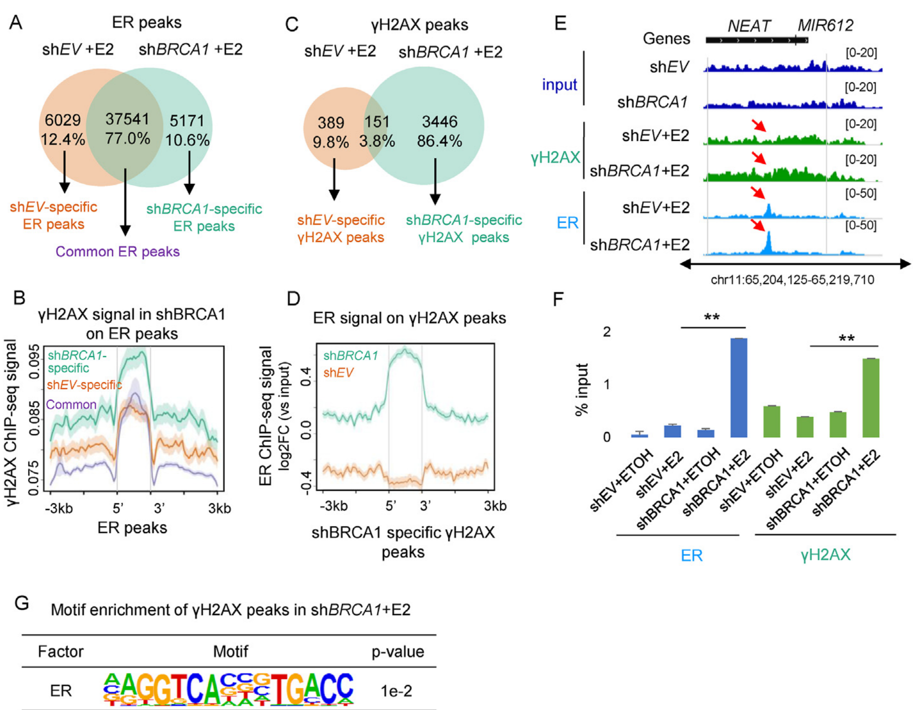

Fig. 2. DNA damage occurs at specific ER binding sites in BRCA1-deficient cells. (A) Venn diagram showing the ER peaks in the E2-treated (10 nM) *shBRCA1* (green) and *shEV* (orange) MCF7 cells. (B) Average read density plots for γH2AX chromatin binding proximal to specific ER binding sites (ERBs) in E2-treated (10 nM) *shBRCA1* MCF7 cells (green), *shEV* MCF7 cells (orange) or common to both (purple). (C) Venn diagram showing the γH2AX peaks in E2-treated (10 nM) *shBRCA1* (green) and *shEV* (orange) MCF7 cells. (D) Average read density plots for ER chromatin binding on *shBRCA1*-specific γH2AX peaks in E2-treated (10 nM) *shBRCA1* MCF7 cells (green) or *shEV* (orange) MCF7 cells. (E) Representative example is given near the *NEAT* locus which shows the profile of γH2AX and ER binding in MCF7 cells treated with E2 (10 nM) or not. (F) ChIP-qPCR assay showing the enrichment of ER and γH2AX near the *NEAT* locus in MCF7 cells treated with E2 (10 nM) or ETOH. (G) Top-enriched transcription factor motifs identified by HOMER at the 3446 γH2AX peaks in E2-treated (10 nM) *shBRCA1* MCF7 cells. (For interpretation of the references to colour in this figure legend, the reader is referred to the Web version of this article.)

BRCA1-knockdown MCF7 cells following E2 treatment. As shown in Fig. 2A, knocking down BRCA1 altered the ER binding profile, and led to an increase in 10.6% of the peaks. Interestingly, the signal of DNA damages on the sh*BRCA1*-specific ER binding sites are higher than that on the *shEV*-specific sites (Fig. 2B). The γH2AX peaks in control and BRCA1-deficient MCF7 cells were also screened, which revealed that ER binding is enriched in *shBRCA1*-specific γH2AX peaks, but not *shEV*-specific γH2AX peaks (Fig. 2C and D). Examples at the *NEAT* and *TAC4 loci by ChIP-qPCR further evidenced this result* (Fig. 2E, F; Supplementary Fig. 2C, D). These findings suggest that γH2AX is correlated with high ER binding after BRCA1 knockdown and E2 treatment. Furthermore, HOMER scanning of the γH2AX peaks in BRCA1-deficient cells showed that the ER motif was enriched in the regions of damaged DNA (Fig. 2G). Taken together, loss of BRCA1 alters the ER binding sites, and increases the frequency DNA damage in the ER-occupied regions.

3.3. *DNA damages are associated with ER-mediated transcriptional activation*

ER is a transcription factor that recruits the co-regulators or other transcription factors to the target gene promoters [12]. Therefore, we hypothesized that the DNA damage induced by strong ER binding is associated with transcriptional activation. Consistent with this, the ER co-activators and active histone markers (H3K27ac and H3K4me1) were enriched in γH2AX peaks in the BRCA1-deficient MCF7 cells after E2 treatment (Fig. 3A). Moreover, the DNA lesions in these cells were highly correlated with the genes expression (Fig. 3B). Knocking down BRCA1 altered the expression levels of E2-responsive genes (Supplementary Figs. 2A and B), and GSEA further showed that genes occupied with γH2AX were enriched in the BRCA1-knockdown as opposed to the control MCF7 cells (Fig. 3C). Furthermore, we observed that the genes with increased expression levels and ER binding after BRCA1 knockdown were more likely to exhibit DNA damage (Fig. 3D). Taken together, BRCA1 deficiency induces genes activation by increasing ER binding, which results in DNA damage.

To confirm the role of ER-dependent transcription in DNA damage induced by E2 stimulation and BRCA1 deficiency, we blocked transcription using the POL II inhibitor 5,6-dichloro-1-β-D-ribofuranosylbenzimidazole (DRB) [13]. The number of γH2AX foci decreased significantly in the E2-treated BRCA1-knockdown cells in response to DRB (Fig. 3E). The POL II inhibitor α-amanitin (αA) [14] also resulted in a similar inhibitory effect on γH2AX foci (Supplementary Fig. 3A). Consistent with the IF results, ChIP-seq showed that DRB treatment significantly decreased the number of γH2AX peaks (Fig. 3F). As confirmed at the *NEAT* and *TAC4 loci, DNA damages were reduced by DRB treatment* (Fig. 3G, H; Supplementary Figs. 3B and C). Taken together, E2-induced DNA damage that is augmented by the loss of BRCA1 is dependent on ER-

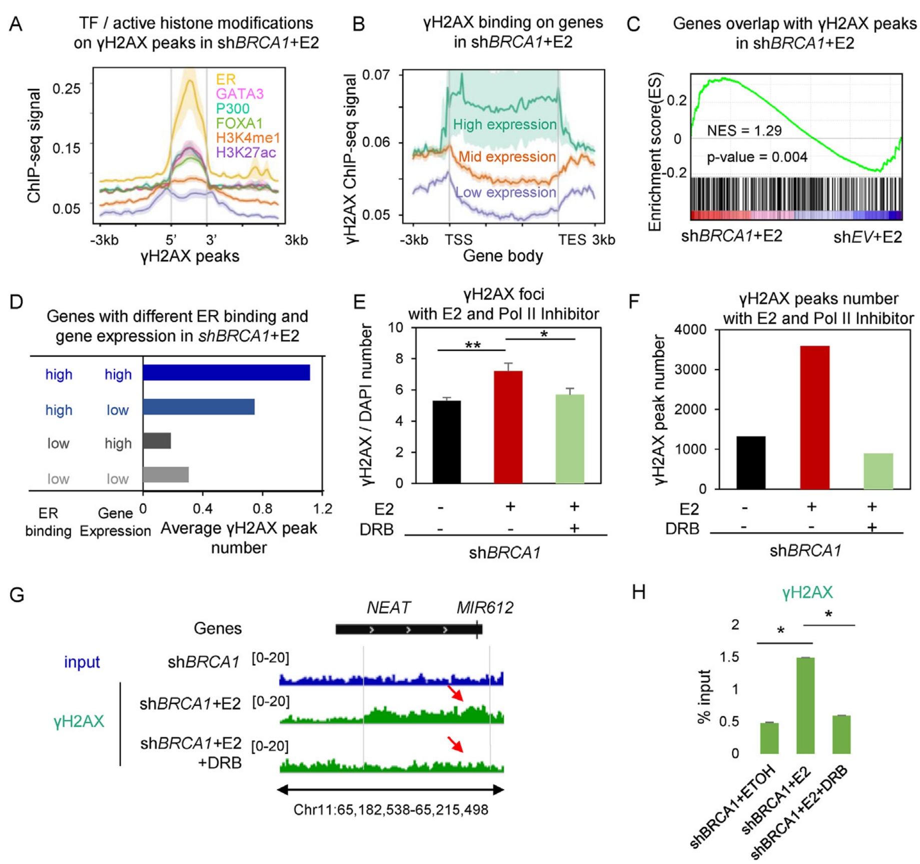

Fig. 3. DNA damage is associated with ER-mediated transcriptional activation. (A) Average read density plots for ER, GATA3, P300, FOXA1, H3K4me1 and H3K27ac chromatin binding on γH2AX peaks in E2-treated (10 nM) *shBRCA1* MCF7 cells. (B) Average read density plots for γH2AX chromatin binding on genes with high, mid and low expression levels in the E2-treated (10 nM) *shBRCA1* MCF7 cells. The total number of genes was 35520. (C) Gene set enrichment analysis (GSEA) of RNA-seq data on genes occupied by total γH2AX peaks in the E2-treated *shEV* or *shBRCA1* MCF7 cells. (D) Number of γH2AX peaks in genes classified on the basis of ER binding and expression levels in the *shEV* and *shBRCA1* MCF7 cells.

(E) Number of γH2AX foci in *shBRCA1* MCF7 cells treated with 5,6-dichloro-1-β-D-ribofuranosylbenzimidazole (DRB, 5 μM), E2 (10 nM) or ETOH. (F) Number of γH2AX peaks in control and *shBRCA1* MCF7 cells treated with DRB (5 μM) and E2 (10 nM). (G) Representative example is given near the *NEAT* loci which shows the profile of γH2AX in MCF7 cells treated with DRB (5 μM), E2 (10 nM) or ETOH. (H) ChIP-qPCR assay showing the enrichment of γH2AX near the *NEAT* loci in MCF7 cells treated with DRB (5 μM), E2 (10 nM) or ETOH.

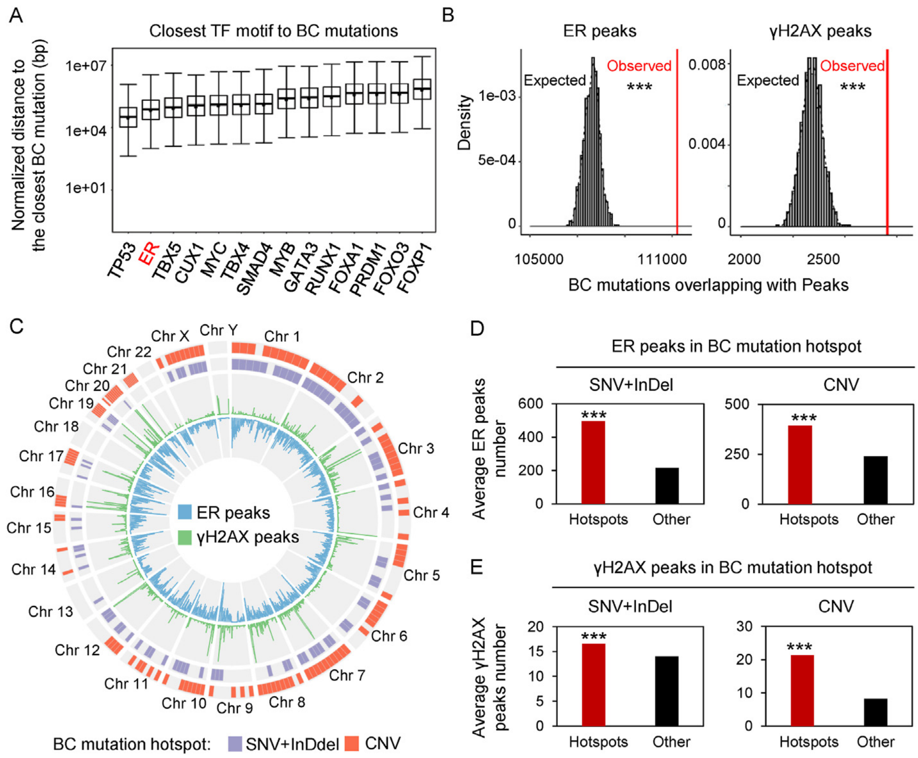

Fig. 4. The damage induced by BRCA1 deficiency and E2 is associated with breast cancer-related mutations
(A) Box plot showing genomic distances between motifs of transcription factor associated with breast cancer and the mutations (SNVs and InDels) in *BRCA1*-mutant breast cancer. (B) Permutation test showing the overlap of ER, γH2AX and random peaks with the SNVs and InDels in *BRCA1*-mutant breast cancer. (C) Circos plot showing enrichment of γH2AX peaks and ER peaks in the regions with mutations of *BRCA1*-mutant breast tumors in E2-treated (10 nM) *shBRCA1* MCF7 cells. Green and blue bars represent the peak density of γH2AX and ER respectively. Each purple tile is a hotpot region with high frequency of SNV and InDel. Each red tile is a hotpot region with high frequency of CNV. (D) Bar plot showing the normalized number of ER peaks in E2-treated (10 nM) *shBRCA1* MCF7 cells inside or outside the hotspots of SNV and InDel (left panel), and inside or outside the hotspots of CNV (right panel) ($p < 0.001$). (E) Bar plot showing the normalized number of γH2AX peaks in E2-treated (10 nM) *shBRCA1* MCF7 cells inside or outside the hotspots of SNV and InDel (left panel), and the hotspots of CNV (right panel) ($p < 0.001$). (For interpretation of the references to colour in this figure legend, the reader is referred to the Web version of this article.)

mediated transcription, and inhibiting the transcriptional pathway can attenuate DNA damage.

3.4. DNA damage induced by BRCA1 deficiency and E2 is associated with breast cancer-related mutations

To assess the clinical relevance of E2-indcued DNA damage, we analyzed the distance between the motifs of breast cancer-associated transcription factors and the clinical mutations in *BRCA1*-mutant breast tumors [15]. The motifs of P53 and ER were closest to these mutations (Fig. 4A). Studies show that the high degree of genomic instability in BRCA1-deficient breast cancer results in frequent mutations in the driver genes of breast cancer [16–18]. We next analyzed the distribution of these mutations, and found that these mutations were significantly enriched in the ER and γH2AX binding sites (Fig. 4B). Moreover, we calculated the mutation hotspots regions in the breast cancer genome using TCGA data, and observed a significant enrichment of γH2AX and ER peaks in hotspots regions of SNPs/Indels and CNVs (Fig. 4C, D, E). As shown in Fig. 4E, the γH2AX peaks were predominantly enriched in the CNVs hotspots compared to the non-hotspot regions (2630 vs 959), which suggests that these DNA damage may be more correlated with CNVs. Taken together, the DNA lesions induced by BRCA1 deficiency and E2 are strongly correlated with the clinical mutations in breast cancer.

4. Discussion

Although it has been widely reported that DNA damage can be induced by E2 treatment, the mechanism of how E2 induces DNA damage in BRCA1-deficient cells, and the relationship between DNA damage and clinical mutations in *BRCA1*-mutant breast tumor are still unclear. In this study, we found that BRCA1 loss altered chromatin binding of ER, which exacerbated DNA damage by activating E2-mediated transcription. Furthermore, these lesions correlated significantly with the clinical mutations in *BRCA1*-mutated tumors.

Studies show that germline BRCA1 mutations principally develop into breast and ovarian cancers. One possible explanation is that the E2-induced DNA damage cannot be repaired due to BRCA1 deficiency, leading to increased genomic instability and accumulation of mutations [2]. E2 initiates DNA damage by mediating R-loop formation [6] and inducing TOP2B-mediated double strand breaks [4]. However, no study so far has emphasized that the inhibitory effect of BRCA1 on the transcriptional activation of ER contributes to genomic stability induced by E2 [11,19]. In this study, we found that BRCA1 deficiency altered the ER binding regions, and DNA damage was mainly localized to these sites. These findings provide new insights into the mechanism through which BRCA1 deficiency and E2 synergistically induce DNA damage in breast tissues, and also provides a possible explanation for malignant transformation being restricted to estrogen-regulated tissues in BRCA1 mutation carriers.

We performed ChIP-seq for γH2AX in the E2-treated (12 h) control and BRCA1-deficient MCF7 cells, and identified 3597 γH2AX peaks in the BRCA1-deficent group compared to only 540 in the control group. However, a recent study identified more than 10,000 γ-H2AX peaks in wild-type MCF7 cells following transient

E2 stimulation (10 min) [20]. Therefore, we hypothesize that E2-induced DNA damage occurs in ER-activated genes within a small time window, and most of them are repaired within 12 h in the presence of wild type BRCA1. Therefore, the lesions we identified in this study represent the persistent DNA damage that might arise from continuously ER-dependent transcriptional activation, which are repaired by BRCA1 in normal breast epithelium but exacerbated in following loss of BRCA1. Thus, our data may better reflect the accumulation of lesions that likely transform to clinically relevant mutations. Indeed, we found these lesions were correlated to the mutations in BRCA1-mutant tumors. The accumulation of these ER-specific and E2-induced mutations may eventually lead to breast and ovarian carcinogenesis.

Acknowledgments

This research was funded by grants from the National Key Research and Development Program (2017YFA0102800), the National Natural Science Foundation of China (Grant Nos. 31970811, 31771639 and 32170798), the Guangdong Innovative and Entrepreneurial Research Team Program (2016ZT06S029), Guangdong Basic and Applied Basic Research Foundation (2021B1515120063), the Guangdong Regenerative Medicine and Health of Guangdong Laboratory Frontier Exploration Project (2018GZR110105007) to J. D.. The Natural Science Foundation of Guangdong Province, China (2021A1515010938) to J.S..

Author contributions

J.C., J.L., P.F., and C.Z., conceived the experiments; P.Z., J.C., and J.S., performed data analysis and statistical calculation; J.C., J.W., W.C., X.L., and J.L., prepared the manuscript; J.D. supervised the project; J.D. funding acquisition.

Declaration of competing interest

We declare that we do not have any commercial or associative interest that represents a conflict of interest in connection with the work submitted.

Appendix A. . Supplementary data

Supplementary data to this article can be found online at https://doi.org/10.1016/j.bbrc.2022.04.142.

References

[1] S.A. Narod, W.D. Foulkes, BRCA1 and BRCA2: 1994 and beyond, Nat. Rev. Cancer 4 (2004) 665–676.

[2] R. Roy, J. Chun, S.N. Powell, BRCA1 and BRCA2: different roles in a common pathway of genome protection, Nat. Rev. Cancer 12 (2011) 68–78.

[3] Chuying Wang, Feng Bai, Li-Han Zhang, Alexandria Scott, Enxiao Li, Xin-Hai Pei, Estrogen promotes estrogen receptor negative BRCA1-deficient tumor initiation and progression, Breast Cancer Res (2018).

[4] H. Sasanuma, M. Tsuda, S. Morimoto, L.K. Saha, M.M. Rahman, Y. Kiyooka, H. Fujiike, A.D. Cherniack, J. Itou, E. Callen Moreu, M. Toi, S. Nakada, H. Tanaka, K. Tsutsui, S. Yamada, A. Nussenzweig, S. Takeda, BRCA1 ensures genome integrity by eliminating estrogen-induced pathological topoisomerase II-DNA complexes, Proc. Natl. Acad. Sci. U. S. A. 115 (2018), E10642-e10651.

[5] J.D. Yager, Mechanisms of estrogen carcinogenesis: the role of E2/E1-quinone metabolites suggests new approaches to preventive intervention–A review, Steroids 99 (2015) 56–60.

[6] C.T. Stork, M. Bocek, M.P. Crossley, J. Sollier, L.A. Sanz, F. Chedin, T. Swigut, K.A. Cimprich, Co-transcriptional R-loops are the main cause of estrogen-induced DNA damage, Elife 5 (2016).

[7] Y.H. Lee, Y. Sun, L.E. Gerweck, R.D. Glickman, Regulation of DNA damage response by estrogen receptor β-mediated inhibition of breast cancer associated gene 2, Biomedicines 3 (2015) 182–200.

[8] A. Rajan, R. Nadhan, N.R. Latha, N. Krishnan, A.V. Warrier, P. Srinivas, Deregulated estrogen receptor signaling and DNA damage response in breast tumorigenesis, Biochimica et biophysica acta, Rev. Cancer 1875 (2021), 188482.

[9] L. Wang, L.J. Di, BRCA1 and estrogen/estrogen receptor in breast cancer: where they interact? Int. J. Biol. Sci. 10 (2014) 566–575.

[10] J. Wang, H. Yu, Q. Ma, P. Zeng, D. Wu, Y. Hou, X. Liu, L. Jia, J. Sun, Y. Chen, D. Guallar, M. Fidalgo, J. Chen, Y. Yu, S. Jiang, F. Li, C. Zhao, X. Huang, J. Wang, C. Li, Y. Sun, X. Zeng, W. Zhang, Y. Miao, J. Ding, Phase separation of OCT4 controls TAD reorganization to promote cell fate transitions, Cell Stem Cell 28 (2021) 1868–1883, e1811.

[11] L. Zheng, L.A. Annab, C.A. Afshari, W.H. Lee, T.G. Boyer, BRCA1 mediates ligand-independent transcriptional repression of the estrogen receptor, Proc. Natl. Acad. Sci. U. S. A. 98 (2001) 9587–9592.

[12] S.C. Hewitt, K.S. Korach, Estrogen receptors: new directions in the new millennium, Endocr. Rev. 39 (2018) 664–675.

[13] M.F. Dubois, V.T. Nguyen, S. Bellier, O. Bensaude, Inhibitors of transcription such as 5,6-dichloro-1-beta-D-ribofuranosylbenzimidazole and isoquinoline sulfonamide derivatives (H-8 and H-7) promote dephosphorylation of the carboxyl-terminal domain of RNA polymerase II largest subunit, J. Biol. Chem. 269 (1994) 13331–13336.

[14] T.J. Lindell, F. Weinberg, P.W. Morris, R.G. Roeder, W.J. Rutter, Specific inhibition of nuclear RNA polymerase II by alpha-amanitin, Science (New York, N.Y.) 170 (1970) 447–449.

[15] E. Zacksenhaus, J.C. Liu, Z. Jiang, Y. Yao, L. Xia, M. Shrestha, Y. Ben-David, Transcription factors in breast cancer-lessons from recent genomic analyses and therapeutic implications, Adv. Protein Chem. Struct. Biol. 107 (2017) 223–273.

[16] H. Davies, D. Glodzik, S. Morganella, L.R. Yates, J. Staaf, X. Zou, M. Ramakrishna, S. Martin, S. Boyault, A.M. Sieuwerts, P.T. Simpson, T.A. King, K. Raine, J.E. Eyfjord, G. Kong, Å. Borg, E. Birney, H.G. Stunnenberg, M.J. van de Vijver, A.L. Børresen-Dale, J.W. Martens, P.N. Span, S.R. Lakhani, A. Vincent-Salomon, C. Sotiriou, A. Tutt, A.M. Thompson, S. Van Laere, A.L. Richardson, A. Viari, P.J. Campbell, M.R. Stratton, S. Nik-Zainal, HRDetect is a predictor of BRCA1 and BRCA2 deficiency based on mutational signatures, Nat. Med. 23 (2017) 517–525.

[17] P. Polak, J. Kim, L.Z. Braunstein, R. Karlic, N.J. Haradhavala, G. Tiao, D. Rosebrock, D. Livitz, K. Kübler, K.W. Mouw, A. Kamburov, Y.E. Maruvka, I. Leshchiner, E.S. Lander, T.R. Golub, A. Zick, A. Orthwein, M.S. Lawrence, R.N. Batra, C. Caldas, D.A. Haber, P.W. Laird, H. Shen, L.W. Ellisen, A.D. D'Andrea, S.J. Chanock, W.D. Foulkes, G. Getz, A mutational signature reveals alterations underlying deficient homologous recombination repair in breast cancer, Nat. Genet. 49 (2017) 1476–1486.

[18] S. Nik-Zainal, H. Davies, J. Staaf, M. Ramakrishna, D. Glodzik, X. Zou, I. Martincorena, L.B. Alexandrov, S. Martin, D.C. Wedge, P. Van Loo, Y.S. Ju, M. Smid, A.B. Brinkman, S. Morganella, M.R. Aure, O.C. Lingjærde, A. Langerød, M. Ringnér, S.M. Ahn, S. Boyault, J.E. Brock, A. Broeks, A. Butler, C. Desmedt, L. Dirix, S. Dronov, A. Fatima, J.A. Foekens, M. Gerstung, G.K. Hooijer, S.J. Jang, D.R. Jones, H.Y. Kim, T.A. King, S. Krishnamurthy, H.J. Lee, J.Y. Lee, Y. Li, S. McLaren, A. Menzies, V. Mustonen, S. O'Meara, I. Pauporté, X. Pivot, C.A. Purdie, K. Raine, K. Ramakrishnan, F.G. Rodríguez-González, G. Romieu, A.M. Sieuwerts, P.T. Simpson, R. Shepherd, L. Stebbings, O.A. Stefansson, J. Teague, S. Tommasi, I. Treilleux, G.G. Van den Eynden, P. Vermeulen, A. Vincent-Salomon, L. Yates, C. Caldas, L. van't Veer, A. Tutt, S. Knappskog, B.K. Tan, J. Jonkers, Å. Borg, N.T. Ueno, C. Sotiriou, A. Viari, P.A. Futreal, P.J. Campbell, P.N. Span, S. Van Laere, S.R. Lakhani, J.E. Eyfjord, A.M. Thompson, E. Birney, H.G. Stunnenberg, M.J. van de Vijver, J.W. Martens, A.L. Børresen-Dale, A.L. Richardson, G. Kong, G. Thomas, M.R. Stratton, Landscape of somatic mutations in 560 breast cancer whole-genome sequences, Nature 534 (2016) 47–54.

[19] C.M. Eakin, M.J. Maccoss, G.L. Finney, R.E. Klevit, Estrogen receptor alpha is a putative substrate for the BRCA1 ubiquitin ligase, Proc. Natl. Acad. Sci. U. S. A. 104 (2007) 5794–5799.

[20] M. Periyasamy, H. Patel, C.F. Lai, V.T.M. Nguyen, E. Nevedomskaya, A. Harrod, R. Russell, J. Remenyi, A.M. Ochocka, R.S. Thomas, F. Fuller-Pace, B. Gyorffy, C. Caldas, N. Navaratnam, J.S. Carroll, W. Zwart, R.C. Coombes, L. Magnani, L. Buluwela, S. Ali, APOBEC3B-Mediated cytidine deamination is required for estrogen receptor action in breast cancer, Cell Rep. 13 (2015) 108–121.